Life Sciences 232 (2019) 116647

Contents lists available at ScienceDirect

Life Sciences

journal homepage: www.elsevier.com/locate/lifescie

Borneol alleviates brain injury in sepsis mice by blocking neuronal effect of endotoxin

Lei Wang, Qiao Liang, Anqi Lin, Yongzheng Wu, Haiyan Min, Shiyu Song, Yong Wang, Hongwei Wang, Long Yi, Qian Gao*

Center for Translational Medicine and Jiangsu Key Laboratory of Molecular Medicine, Medical School of Nanjing University, Nanjing, 210093, Jiangsu Province, China

ARTICLE INFO

Keywords:
Borneol
Sepsis
Neuroinflammation
Neuroprotection
MAPK signaling

ABSTRACT

Aim: Brain injury after sepsis leads to high mortality and long-term brain dysfunction in patients. Previous studies revealed that borneol has a protective effect on the brain, but its function on sepsis associated encephalopathy (SAE) remains unknown. Herein, we investigated the protective effect of borneol against sepsis-related brain injury.

Main methods: Lipopolysaccharide (LPS)-induced sepsis mice and cells were treated with borneol at the dose of 100 mg/kg by gavage or 10 μg/ml in culture, respectively. The protective effect of borneol on neurons and the microglia were assessed *in vivo* and *in vitro*.

Key findings: We observed that borneol attenuated brain neuronal and microglial inflammation in LPS-induced sepsis mice with a suppression of p-p65 and p38 signaling that were initially activated by LPS in the brain. *In vitro* examination confirmed that the protective effect of borneol on both neurons and microglia, and its suppressive effect on p-p65 and p38 pathways were, at least in part, direct.

Significance: An early protection of neurons and microglia from bacterial endotoxin during sepsis is beneficial, and borneol has the potential to protect these cells.

1. Introduction

Sepsis is a life-threatening condition that often leads to multiple organ dysfunctions and is a major cause of death for patients in intensive care clinics [1]. Sepsis-associated encephalopathy (SAE), a condition of inflammatory brain injury, has been reported to occur earlier and more frequently than peripheral organ damages during the development of sepsis [2]. It affects all brain cells and causes neuron dysfunction and apoptosis, microglia activation and intracellular metabolic disorders [3], which worsens the overall conditions of sepsis in acute phase and results in long-term impairment of brain function on septic survivors [4]. In fact, clinically, the severity of sepsis is often diagnosed by measuring the extent of SAE, manifested mainly as Glasgow Coma Scale (GCS) scoring in mental states from mild confusion, delirium to coma [5], therefore, an early treatment of SAE is essential in improving the prognosis of patients with sepsis [6].

The mechanism of SAE is highly complex, involving the blood-brain-barrier (BBB) breakdown and systemic cytokine invasion of the brain, which triggers severe neuroinflammation, neurotransmitter imbalance and cerebral blood flow dysregulation, according to recent views [3,5,6]. The direct effect of bacterial endotoxin on the brain, affecting both neurons and microglia, in the early phase of sepsis should not be dismissed [7] as it may be the early trigger of neuroinflammation in SAE, which was overserved in LPS-induced sepsis models [8,9].

Traditionally, the treatment of sepsis is mainly supportive, including controlling infection, sustaining organ functions, and maintaining metabolic homeostasis mainly at systemic level [7]. However, the consequence of this approach is not satisfactory, particularly in blocking acute neuronal damage, which is crucial in stopping further development of sepsis and preventing long-term brain dysfunction in sepsis survivors. Thus, there is a clinical need for developing new means of neuronal protection in addition to infection control in the early stage of sepsis.

Borneol, a bicyclic monoterpene, is a time-honored herb in traditional Chinese medicine using for “waking up” the brain [10]. It was suggested to be protective against brain injury in clinical brain ischemic stroke [11] and cognitive impairment in cerebral ischemia mice [12]. Moreover, it was believed to effectively facilitate the transportation across the blood-brain-barrier (BBB) [13] and has neuroprotective effect in Alzheimer's disease [14]. However, the mechanisms underlying

* Corresponding author.
E-mail address: qian_gao@nju.edu.cn (Q. Gao).

https://doi.org/10.1016/j.lfs.2019.116647
Received 1 March 2019; Received in revised form 26 June 2019; Accepted 9 July 2019
Available online 10 July 2019
0024-3205/

its neuronal protection against brain injury remain unclear. Further, few studies have examined the role of borneol in SAE.

Herein, we set to ask whether borneol protects against sepsis-induced encephalopathy in an LPS-induced mouse model. We found that borneol significantly reduced brain inflammation and neuronal toxicity in the early stage of sepsis; judged by a significant increase of early survival rate of animals and a strong reduction of neuroinflammatory pathology in the brain of sepsis mice. Moreover, we showed that the protective effect of borneol on neurons is, at least in part, direct as it efficiently suppressed the neuronal toxicity of LPS *in vitro*. The molecular mechanism underlying the neuronal protection of borneol was also explored. SAE related signaling, NF-κb and MAPK pathways [15,16], were blocked by borneol *in vivo* and *in vitro*. Our findings emphasized the importance of early neuroprotection in severe infectious disease and offer new possibilities for clinical treatment of sepsis.

2. Materials and methods

2.1. Animal experimental procedure

Specific pathogen-free (SPF) male C57BL/6J mice (5–6-week-old) weighting 20–25 g were obtained from Model Animal Genetics Research Center of Nanjing University (Nanjing, China). Animal welfare and experimental procedures were carried out strictly in accordance with the Guide for the Care and Use of Laboratory Animals (Nanjing University). Mice were acclimated for at least a week before use. All mice were housed in specific pathogen free (SPF) condition with a 12:12 h light-dark cycle, and received water and food *ad libitum*.

LPS-induced sepsis was established by intraperitoneal injection. LPS (from *Escherichia coli* 055: B5) and borneol were from Sigma Chemical Co. (St. Louis, USA). The experiments were carried out in the following groups: Sham group (intraperitoneal injection of PBS), LPS group (20 mg/kg LPS, intraperitoneal injection [17–19]), LPS + Borneol group (intragastrical administration of borneol at the dose of 100 mg/kg/day [20] after LPS challenge for 5 days), and Borneol group (intragastrical administration of borneol at the dose of 100 mg/kg/day for 5 days). Every group has least 6 mice. The survival studies were conducted over 7 days.

2.2. Enzyme linked immunosorbent assay (ELISA)

ELISA Double Sandwich Method was used to detect the inflammatory cytokines in the brain tissues of mice. After the brain tissue supernatant was obtained by tissue homogenization using phosphate buffer saline, the samples and standards were mixed with the previously coated monoclonal antibodies on the microplate to form an immune complex (Research&Diagnostics Systems , Inc. Minneapolis, USA), and the tissue debris were washed away. An additional biotinylated antibody was then added to form a sandwich with the initial immune complex and the free component was washed away. Horseradish peroxidase-labeled avidin was added, and avidin and biotin were specifically combined, and the free component was washed away. Finally, the chromogenic substrate was added, and the horseradish peroxidase turned the color developer into blue. After the addition of the stop solution, it turned yellow, and the optical density (OD) value was measured at the wavelength of 450 nm by BioTek ELx800 automatic microplate reader (BioTek, Vermont, USA). The concentration of the inflammatory factor was determined by comparing to a standard curve.

2.3. Histological analysis and immunohistochemistry

After the mice were anesthetized, we used normal saline to perfuse the animals at the position of the left ventricle of the heart until the color of the liver and lung turned white. We then used 4% paraformaldehyde to perfuse until the limbs of mice became stiff. The fixed brains were quickly taken and fixed in 4% paraformaldehyde for additional 24 h followed by saline wash (24 h at 4 °C) and embedded in paraffin, sectioned into 7 μm slices for staining. For Low or high magnification images of mouse brain slices, immunofluorescence staining for neuronal or glial markers in the brains of different group mice were performed. The slides were blocked with goat serum and incubated with primary antibody NeuN (ABN78) (Millipore, Boston, USA), Iba1 (ab5076) and MAP2 (ab32454) (Abcam, Cambridge, UK), overnight at 4 °C. Alexa Fluor 594 (Invitrogen, Carlsbad, USA) was used as the secondary antibody in immunofluorescence assays. 2% BSA (diluted in PBS) was used as dilution factor for IHC and ICC. For Low magnification images, the brain slices were prepared at the Coronal 47–50 level according to Allen Reference Atlas (or Plate 21–23 level according to George Paxinos & Keith B. J. Frankelin's the Mouse Brain in Stereotaxic Coordinates). The Olympus IX73 inverted microscope (Olympus, Tokyo, Japan) with 4× objective was used to taken images. The interested target areas were customized and the entire sectioned areas were scanned and composed using cellSens Dimension1.17; exposure time 1 s. For high magnification images, the pictures of tissue immunofluorescence were captured by confocal microscopy (Olympus, Tokyo, Japan).

For microglia activation assay, Iba-1 staining was performed, which illustrated both activated as well as non-activated microglia with very different morphology. The activated microglia exhibited enlarged amoebic shape. The Image J software (NIH, Bethesda, MD, USA) was used to convert fluorescence, and bright-field photomicrographs was used into representative binary and skeletonized images that were further analyzed using software plugins Analyze Skeleton (2D/3D) and FracLac for morphology data collection [21]. The outcomes of the plugins summarize the cell morphology in terms of the process length, junctions and endpoints, as well as cell complexity, shape, and size descriptors. Upon the morphological information, the activated microglia were identified and quantified [21,22].

2.4. Cell culture and purity assay

For primary microglia, 1 or 2-day old C57BL/6 mice were used. The animals were sacrificed by cervical dislocation. The brains were removed and the entire cortex of individual mouse was isolated in Leibovitz's L15 medium (Gibco Life Technologies, New York, USA). The tissue was dissociated by the nylon membrane (pore size of 70 mu m cell filter; Falcon, Pittsburgh, USA) mechanically. After centrifugation, the precipitates were suspended in Dulbecco's modified Eagle's medium, 10% fetal bovine serum and 1% gentamicin (Gibco Life Technologies, New York, USA). Cells were cultured in 5% CO_2 at 37 °C, and medium was half-changed at day 5. Two weeks later, flasks were shaken gently and microglia was collected.

For primary neuronal cultures, the tissues of cerebral cortex were obtained from E16–17 mouse embryos. The cultures were kept in 5% CO_2 at 37 °C and fed beginning from the fourth day with cultivating medium by replacing half of the medium twice a week, and were used for experiments after 7 days.

The purity of cultured cortical neurons (MAP2 positive) was determined by immunofluorescence staining of microglia (Iba-1) and astrocyte (GFAP), respectively, and counted under a regular fluorescence microscopy (Olympus, Tokyo, Japan). Each staining was prepared in triplicate. The labeled cells in two independent microscopic views for each well that was specifically labeled by either Iba-1 or GFAP were counted and presented as the percentage of the total cells ($MAP2^+ + Iba\text{-}1^+$ or $MAP2^+ + GFAP^+$, respectively) in each view. The purity of the neuronal preparations met the requirement of > 95%. The representative images for each staining were presented.

2.5. Western blot

For whole protein extraction, the brain cortex (at the same quality 20 mg) or cells (microglia or neurons, 10^6/well) was prepared by adding radioimmunoprecipitation assay (RIPA) buffer (Beyotime Institute of Biotechnology, Nanjing, China) containing protease inhibitors and phosphatase inhibitors cocktail (Thermo Scientific, USA), and quantified with Thermo Scientific BCA kit (USA). For nuclear or cytoplasmic protein extraction, NE-PER Nuclear and Cytoplasmic Extraction Reagents (Thermo Pierce, USA) was used for nucleo-cytoplasmic separation (microglia and neurons). In brief, 100 μl Reagent A was added to the cells (10^6) for 20 min, centrifuged for 10 min at 3000*g* at 4 °C, and the supernatant was collected, then 150 μl Reagent B was added to the sediment for 20 min, centrifuged for 10 min at 12,000*g* at 4 °C, the supernatant was collected. Equal amount of proteins from each sample was separated by SDS-PAGE and blotted onto polyvinylidene fluoride (PVDF) membrane, and incubated with appropriate antibody over night at 4 °C. After washing, the membrane was incubated at room temperature with horseradish peroxidase-conjugated anti-rabbit IgG for 90 min and the result was visualized using the ECL Plus western blotting detection reagents (Millipore, UA). We used GAPDH (#5174, dilution 1:1000), ERK (#4695, dilution 1:1000), Phospho-ERK (#4370, dilution 1:1000), p38 (#8690, dilution 1:1000), Phospho-p38 (#4511, dilution 1:1000), Laminb1 (#13435, dilution 1:1000), NF-κB/p65 (#8242, dilution 1:1000), Phospho-NF-κB/p-p65 (#3033, dilution 1:1000), Phospho-SAPK/JNK (#4668, dilution 1:1000) and SAPK/JNK (#9252, dilution 1:1000) antibodies purchased from Cell Signaling Technology (Danvers, Boston, Massachusetts. USA) for Western Blot. CD16 (#ab203883, dilution 1:1000) and CD206 (#ab125028, dilution 1:1000) antibodies were purchased from Abcam (Cambridge, UK). Protein GAPDH was used as an internal control. The intensities of bands (relative protein levels) were quantified by densitometry using ImageJ software (NIH, Bethesda, MD, USA).

2.6. Quantitative real-time polymerase chain reaction (qPCR)

Total RNA was isolated from tissue samples and cells using Trizol reagent and first-strand complementary DNA (cDNA) was synthesized using iScript cDNA Synthesis Kit (Vazyme, Nanjing, China). Quantitative PCR (qPCR) was performed with SYBR green PCR Master Mix (Vazyme, Nanjing, China) using viia 7 Real-Time PCR System (Applied Biosystems, Waltham, CA). The primers used in this work were listed in Table 1. In each qPCR experiment, the same samples were performed in triplicate and the same experiment was performed at least three times. The quantification of the qPCR results was achieved by a comparative method $2^{-\Delta\Delta CT}$ ($2^{-[\text{experiment group (CT of target gene - CT of actin) - control group (CT of target gene - CT of actin)}]}$) using β-actin as an internal control (the calibrator) from the respective control animals or cells.

2.7. Cell viability assessment

After treated with microglia-free supernatants for 24 h, cell counting kit-8 (CCK-8) analysis (Sigma, St. Louis, USA) and LDH release assay (Beyotime Biotechnology, Shanghai, China) were used to measure the viability of neurons (Four wells for each group). For CCK-8 analysis, 10 μl CCK-8 solution (5 mg/ml) were added into each well (96-well) and incubated at 37 °C for 2 h. The absorbance at 450 nm was measured with a microplate reader (BioTek, Vermont, USA). The cell viability is defined as [(Experiment well absorbance - blank well absorbance) / (Control well absorbance - blank well absorbance)] × 100%; Where experimental well included testing cells, medium, CCK-8 with LPS, LPS + borneol or borneol alone, respectively; Control well included testing cells, medium, CCK-8, without LPS or borneol; Blank well included medium, CCK-8 with no cells and LPS or borneol. The cell death percentage was calculated as (1-cell viability).

For LDH release analysis, the cells were seeded into 96-well cell culture plates. The culture solution was washed with PBS and changed with fresh culture medium, and each culture well was divided into the following groups: background blank control well, sample control well, sample maximum enzyme activity control well, and drug treatment sample well (n = 4). One hour before scheduled detection time point, LDH release reagent (10% of the volume of the culture solution) was added to the sample maximum enzyme activity control well, and then continued to incubate in the cell culture incubator. After 24 h, it was centrifuged for 5 min at 400*g*. 120 μl supernatant of each well was taken for sample measurement. The dual wavelength absorbance was then measured with a microplate reader (BioTek, Vermont, USA) at 490 nm as experimental absorption measurement and the 650 nm as the reference absorption. The toxicity of LDH was calculated by A490 nm - A650 nm.

Calcein-AM/PI double stain kit (Yeasen biotech Co., Shanghai, China) was used and the cell suspension was prepared using assay buffer to a density of 1×10^5 to 1×10^6 cells/ml, 100 μl of the staining working solution (2 μM Calcein-AM and 4.5 μM PI) was added to 200 μl of the cell suspension, then mixed and incubated at 37 °C for 15 min. Viable cells (yellow-green fluorescence) and dead cells (red fluorescence) were simultaneously detected using a 490 ± 10 nm excitation filter under a fluorescence microscope (Olympus, Tokyo, Japan) and counted by eyes. Three independent wells for each group were averaged.

2.8. Data analysis

Experimental data were analyzed using SPSS 13.0 software, two-way ANOVA and multiple comparisons followed by Tukey were used when two factors were involved. Data were expressed as the Mean ± SEM (standard error of the mean), all statistical tests were two-sided with $P < 0.05$ considered statistically significant.

Table 1
Primers of mice used for real-time quantitative PCR analysis.

Gene	Forward primer	Reverse primer
β-Actin	GGACGTACAACTGGTATTGTGC	TCGGCAGTAGTCACGAAGGA
IL-10	AGCCTTATCGGAAATGATCCAGT	GGCCTTGTAGACACCTTGGT
TNF-α	CAGGCGGTGCCTATGTCTC	CGATCACCCCGAAGTTCAGTAG
IL-1β	GCAACTGTTCCTGAACTCAACT	ATCTTTTGGGGTCCGTCAACT
IL-6	TAGTCCTTCCTACCCCAATTTCC	TTGGTCCTTAGCCACTCCTTC
CD11b	ATGGACGCTGATGGCAATACC	TCCCCATTCACGTCTCCCA
CD16	CAGAATGCACACTCTGGAAGC	GGGTCCCTTCGCACATCAG

3. Results

3.1. Borneol protected neuroinflammation in sepsis mice

The survival curve showed that borneol treatment (100 mg/kg) delivered an early protective effect on LPS (20 mg/kg) induced damage judged by a significant reduction of mortality of sepsis mice in the early (between 24 h to 72 h) stage (Fig. 1A). To investigate whether this effect of borneol is related to the brain protection in LPS-induced sepsis, immunofluorescence was used to observe the survival of neurons in the cerebral cortex (Materials and methods). As shown in Fig. 1B, large numbers of cortical neurons exhibited loss of NeuN label after LPS insult, indicating a severe neuronal damage. The low magnification images of mouse brain slices showed that LPS' toxic effect was broad, affecting large areas of the brain cortex and internal capsule (Supplement Fig. 1). Borneol greatly reduced this damage in sepsis mice. In contrast, there was a significant activation of microglia revealed by a widely increased number of high Iba1 labeled amoebic microglia, which illustrated the responding resident microphages in the central nervous system [23]. Again, borneol greatly reduced the number of amoebic microglia in the cortex in sepsis mice (Fig. 1E). In consistent,

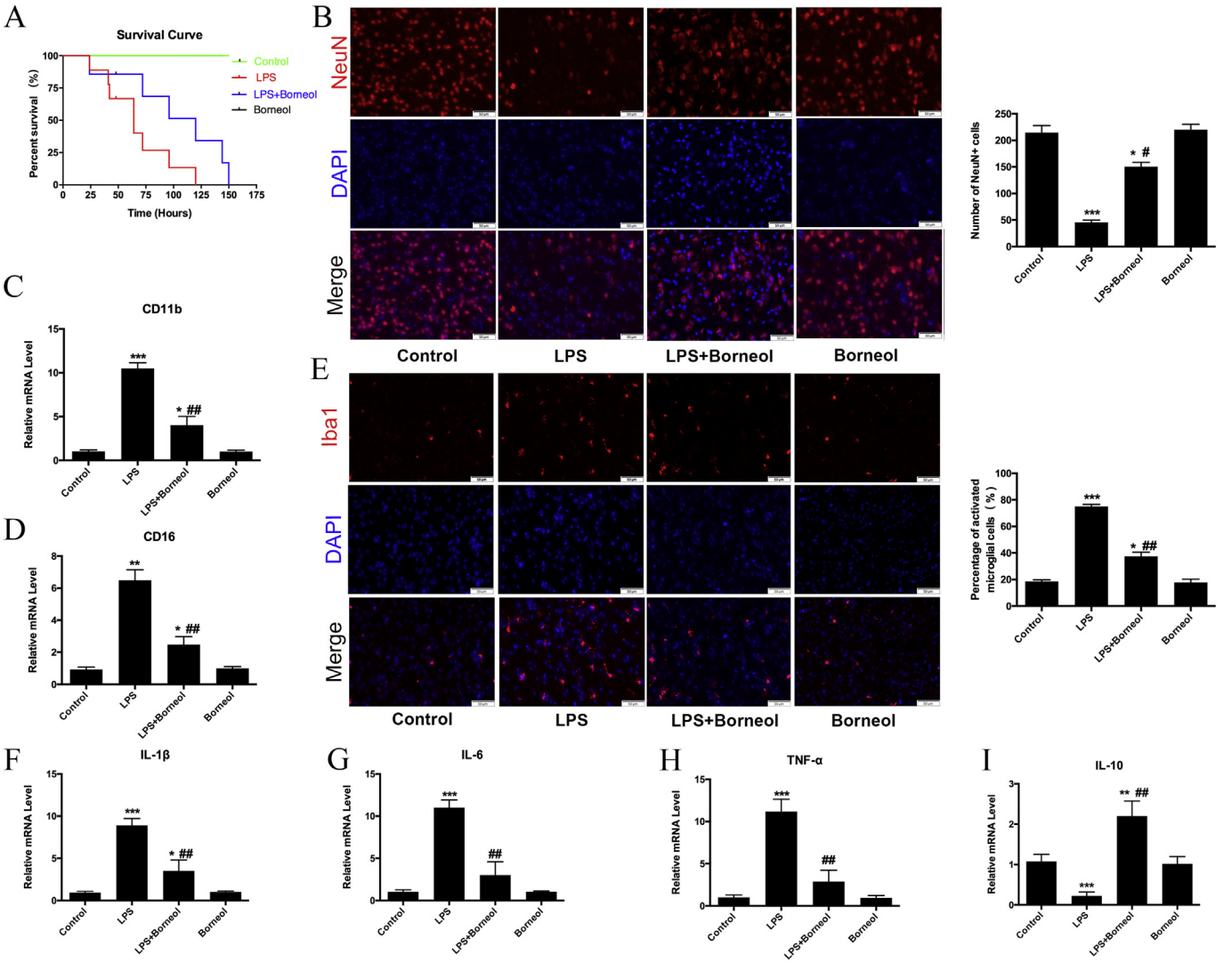

Fig. 1. Borneol protected neuroinflammation in septic mice. (A) The survival curve of mice after LPS challenge. The survival time is indicated as hours that the animal's survival after LPS-exposure. (B) Immunofluorescence staining and quantification for NeuN expression in the brain cortex of mouse (Scale bar: 50 μm). (C, D) The mRNA levels of pro-inflammatory microglia marker *CD11b* and *CD16* in the brain examined by RT-qPCR. (E) Immunofluorescence staining and quantification for Iba1 expression in the brain cortex of mouse (Scale bar: 50 μm). (F–I) The mRNA levels of *IL-1β*, *IL-6*, *TNF-α* and *IL-10* in the brain cortex determined by q-PCR. (B–I) In all experiments, the animals were sacrificed 24 h after LPS exposure. Data were expressed as mean ± SEM, n = 6, *P < 0.05, **P < 0.01, ***P < 0.001 compared with the Control group. $^{\#}$P < 0.05, $^{\#\#}$P < 0.01, $^{\#\#\#}$P < 0.001 compared with the LPS group.

the markers of pro-inflammatory microglia, *CD11b* and *CD16*, were upregulated upon LPS-induction, but reversed by borneol determined by RT-qPCR (Fig. 1C, D). The levels of pro-inflammatory cytokine *TNF-α*, *IL-1β* and *IL-6* were also significantly increased in the brain after LPS challenge, and the level of anti-inflammatory cytokine *IL-10* was dramatically decreased, which were reversed by borneol treatment (Fig. 1F–I). No obvious difference between control and borneol groups was observed, indicating no significant cellular toxicity of borneol. Thus, borneol protected neuroinflammation in sepsis mice.

3.2. Direct suppression of microglia activation by borneol in vitro

To test whether borneol's protective effect on microglia activation was direct, we set to evaluate the cellular effect of borneol on microglia *in vitro*. As shown in Fig. 2A&B, the microglia initially isolated from cerebral cortex were activated after LPS (100 ng/ml, 24 h) challenge, revealed as the increase of the numbers of Iba1 high expression cells [23], which was greatly reduced by borneol (10 μg/ml, 24 h). Consistently, the protein expression of CD16 was significantly increased after LPS challenge and it was reversed by borneol treatment (Fig. 2C). In contrast, the protein level of CD206, an anti-inflammatory marker of microglia, was notably reduced after LPS, and it was again reversed by the treatment of borneol (Fig. 2C&D). We also measured the inflammatory cytokine *IL-1β*, *IL-6* and *TNF-α* secreted by primary microglia after LPS challenge with/without borneol by ELISA. The results were consistent with the *in vivo* observation (Fig. 2E–G). Interestingly, the level of *IL-10* secreted by primary microglia after LPS was not reduced, but slightly elevated, however, in the same setting, borneol significantly increased *IL-10* level (Fig. 2H), suggesting that there was additional mechanism in the brain that contributed to the significant reduction of *IL-10* production by LPS, which was obviously suppressed by borneol treatment (Fig. 1I). Together, borneol directly suppressed LPS-induced inflammation by suppressing the pro-inflammatory cytokine production and facilitated the pro-inflammatory cytokine synthesis in microglia *in vitro*.

3.3. Borneol reduced microglia activation-related neuronal damage in vitro

To investigate the effect of microglia on neurons, the cell-free culture medium of primary microglia that were obtained from 1 or 2-day-

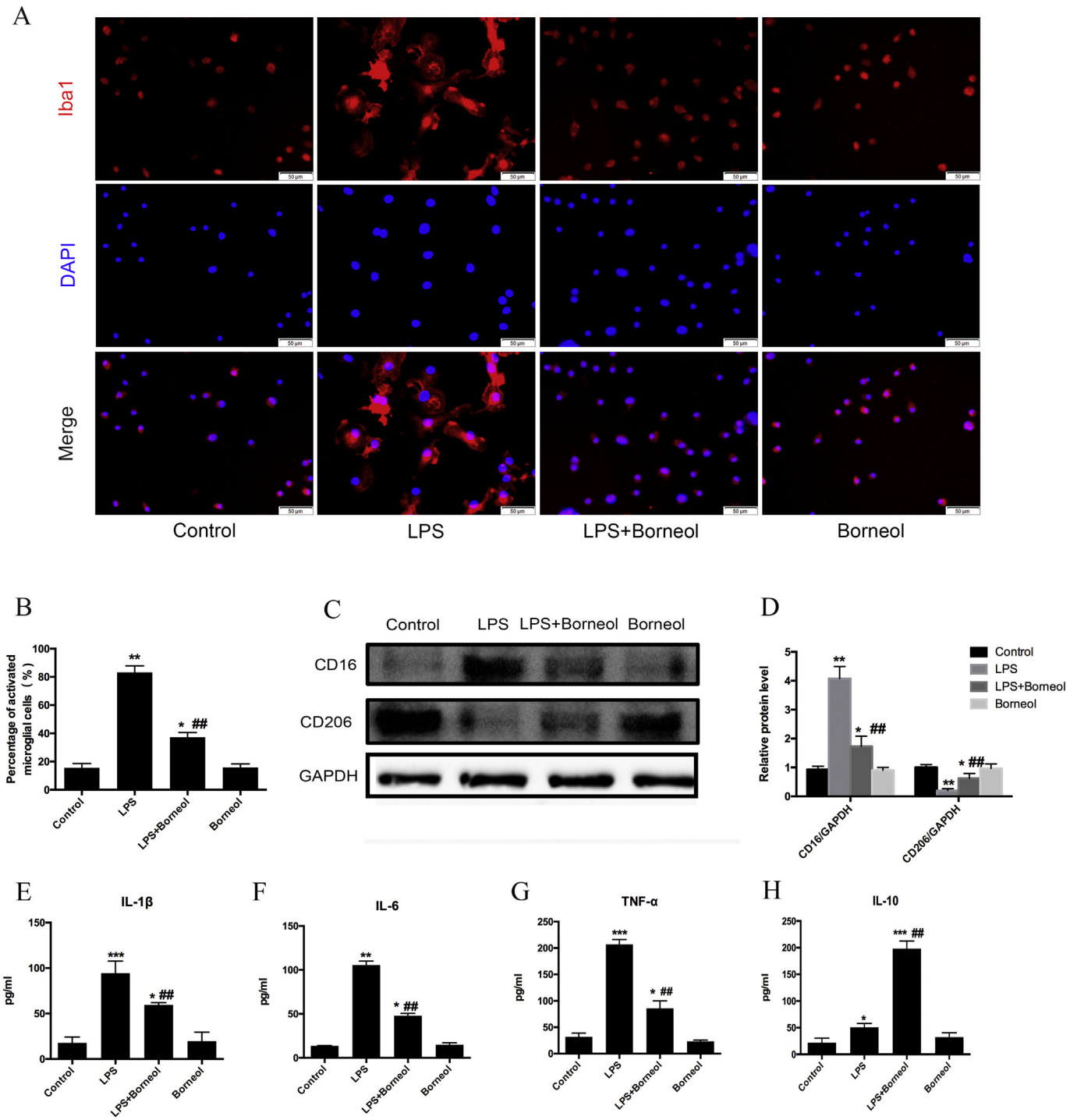

Fig. 2. Direct suppression of microglia activation by borneol *in vitro*. (A, B) Immunofluorescence staining and quantification (percentage of activated microglia) for Iba1 expression in cultured primary microglia isolated from the brain cortex from day 1 or 2 new born mice (Scale bar: 50 μm). (C, D) Western blot analysis and quantification (relative protein level) for CD206 and CD16 expressions in cultured primary microglia. (E–H) The levels of *IL-1β*, *IL-6*, *TNF-α*, and *IL-10* proteins in the supernatant of cultured primary microglia detected by ELISA. The experiments were assayed 24 h after LPS exposure with/without borneol. Data were expressed as mean ± SEM, n = 10. *P < 0.05, **P < 0.01, ***P < 0.001 compared with the Control group. $^{\#}$P < 0.05, $^{\#\#}$P < 0.01, $^{\#\#\#}$P < 0.001 compared with the LPS group.

old new born mice initially challenged by LPS with/without borneol (Materials and methods) were added to neurons that were obtained from E16–17 mice at the ratio of 1:3. The survival status of cultured neurons was assessed 24 h later. Lactate dehydrogenase (LDH) release assay and cell counting analysis showed that neuronal death was increased after the addition of supernatant from activated microglia. However, borneol treated microglia culture medium cancelled the toxicity of activated microglia to neurons (Fig. 3A, B). Calcein-AM/PI double staining, an assay that measures neuron death, confirmed the protective effect of borneol by suppressing the neuronal toxicity of activated microglia (Fig. 3C).

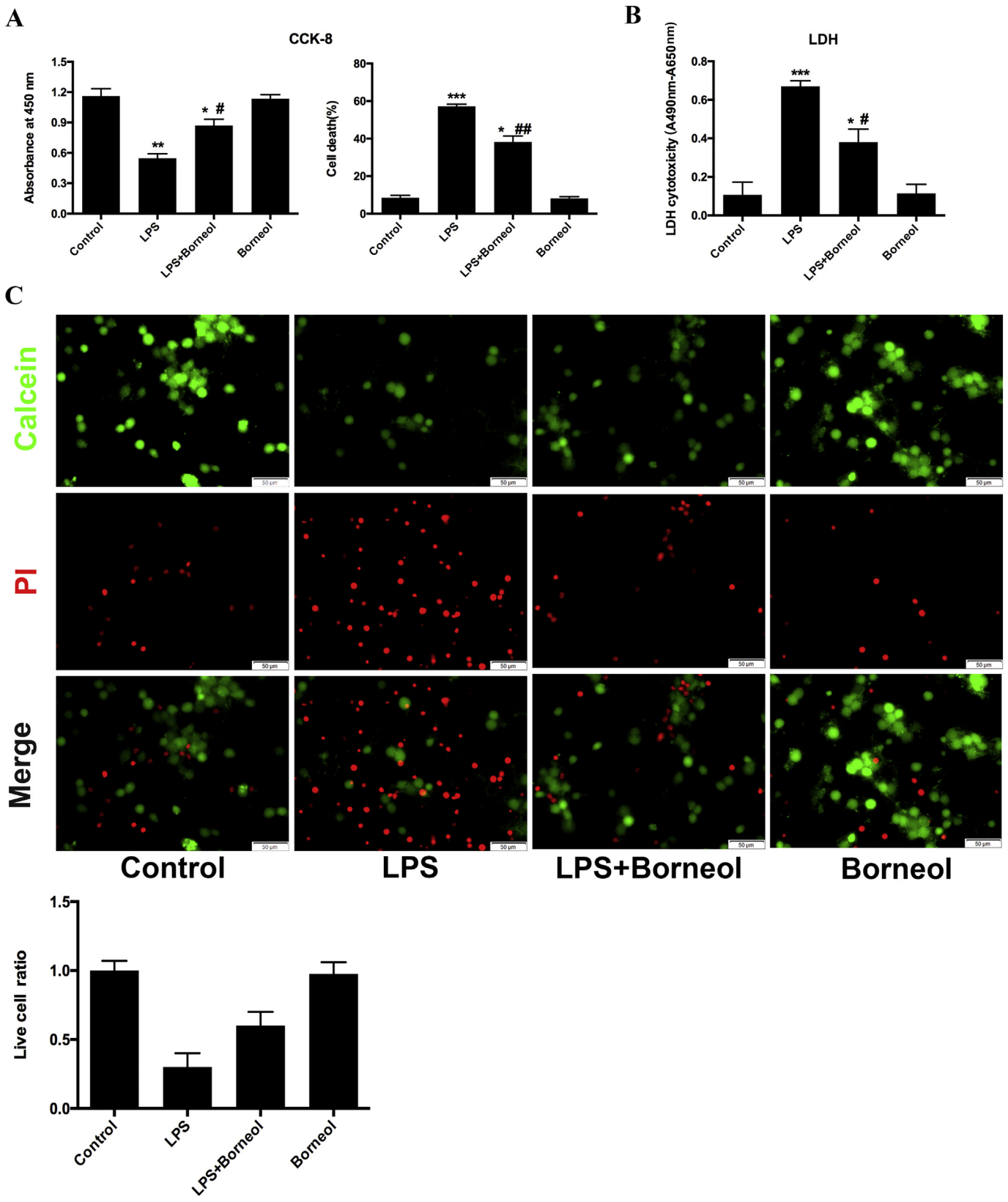

Fig. 3. Microglia related neuronal damage was ameliorated by borneol *in vitro*. (A) Cell counting kit-8 analysis (absorbance and calculated cell death percentage) of neurons measured by the absorbance at 450 nm with a microplate reader. (B) Lactate dehydrogenase (LDH) release assay of neuronal death measured by dual wavelength absorbance (A490 nm-A650 nm) with a microplate reader. (C) Calcein-AM/PI double staining in microglia cells (Scale bar: 50 μm). The quantification was determined by the ratio of live neurons. All experiments were assayed 24 h after the exposures of the supernatants from either activated microglia or from borneol protected microglia. Data were expressed as mean ± SEM.*P < 0.05, **P < 0.01, ***P < 0.001 compared with the control group. ***P < 0.001 compared with the Control group. $^{\#}$P < 0.05, $^{\#\#}$P < 0.01 compared with the LPS group.

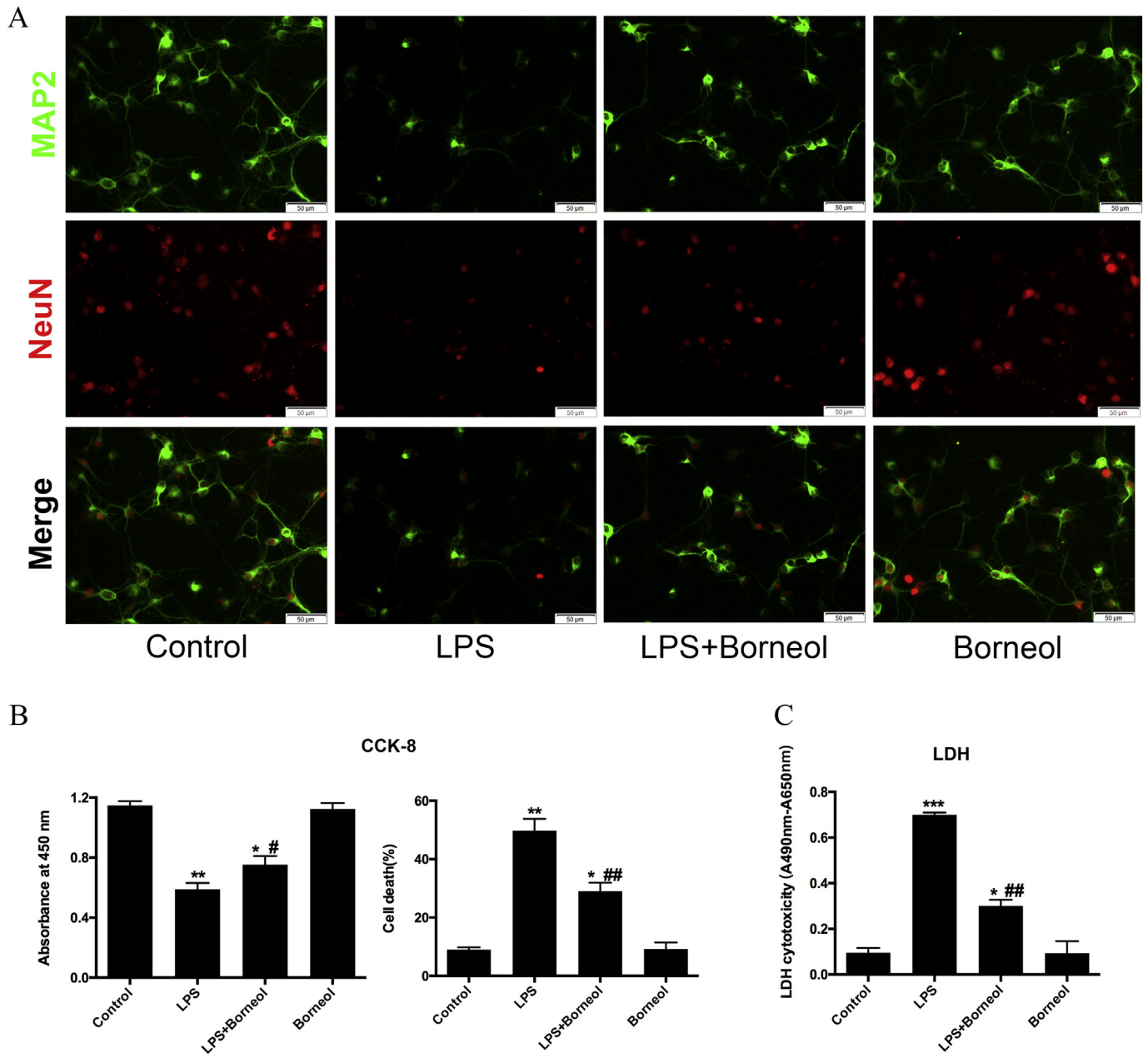

Fig. 4. Borneol directly protected neurons from LPS toxicity. (A) Immunofluorescence staining for NeuN and MAP2 expressions in cultured primary neurons from the brain cortex of E16–17 embryo mice (Scale bar: 50 μm), The nucleus staining of NueN and cellular skeleton labeling of MAP2 were appreciated. (B) Cell counting kit-8 analysis (absorbance and cell death percentage) of neurons measured by the absorbance at 450 nm. (C) Lactate dehydrogenase (LDH) release assay of neuronal death measured by dual wavelength absorbance (A490 nm-A650 nm). All experiments were assayed 24 h after LPS challenge (100 ng/ml) with or without borneol (10 μg/ml). Data were expressed as mean ± SEM.*P < 0.05, **P < 0.01, ***P < 0.001 compared with the control group. ***P < 0.001 compared with the Control group. $^{\#}$P < 0.05, $^{\#\#}$P < 0.01 compared with LPS group.

3.4. Borneol directly protected neurons from LPS toxicity

To test whether LPS toxicity and borneol's protective effect on neurons were both direct at cellular level, we initially isolated and cultured neurons from the cortex of mice (E16–17). The purity of the primary neurons in culture was > 95% (Supplementary Fig. 2). The neuronal biomarker NeuN and microtubule-associated protein 2 (MAP2) were detected. As revealed, both NeuN and MAP2 were greatly reduced 24 h after LPS administration, which was reversed by borneol treatment (10 μg/ml) (Fig. 4A). Consistently, Lactate dehydrogenase (LDH) release assay and cell counting analysis detected severe neuron deaths after LPS challenge, while borneol treatment suppressed this effect of LPS (Fig. 4B, C). Thus, the *in vivo* toxic effect of LPS as well as the protective effect of borneol on neurons were both, at least in part, direct.

3.5. Borneol reduced neuroinflammation by disrupting MAPK signaling pathway

As p65, an innate immune component, participates sterile-inflammation and wound healing [24], and was highly phosphorylated in ischemic stroke-induced brain injury [25], we initially assayed the p65 signaling in LPS treated brain and cells. We found that the phosphorylation of p65 was significantly increased after LPS challenge, while borneol suppressed this effect of LPS (Fig. 5A, B). We then measured the activation of MAPK pathway. As shown in Fig. 5A, the phosphorylation

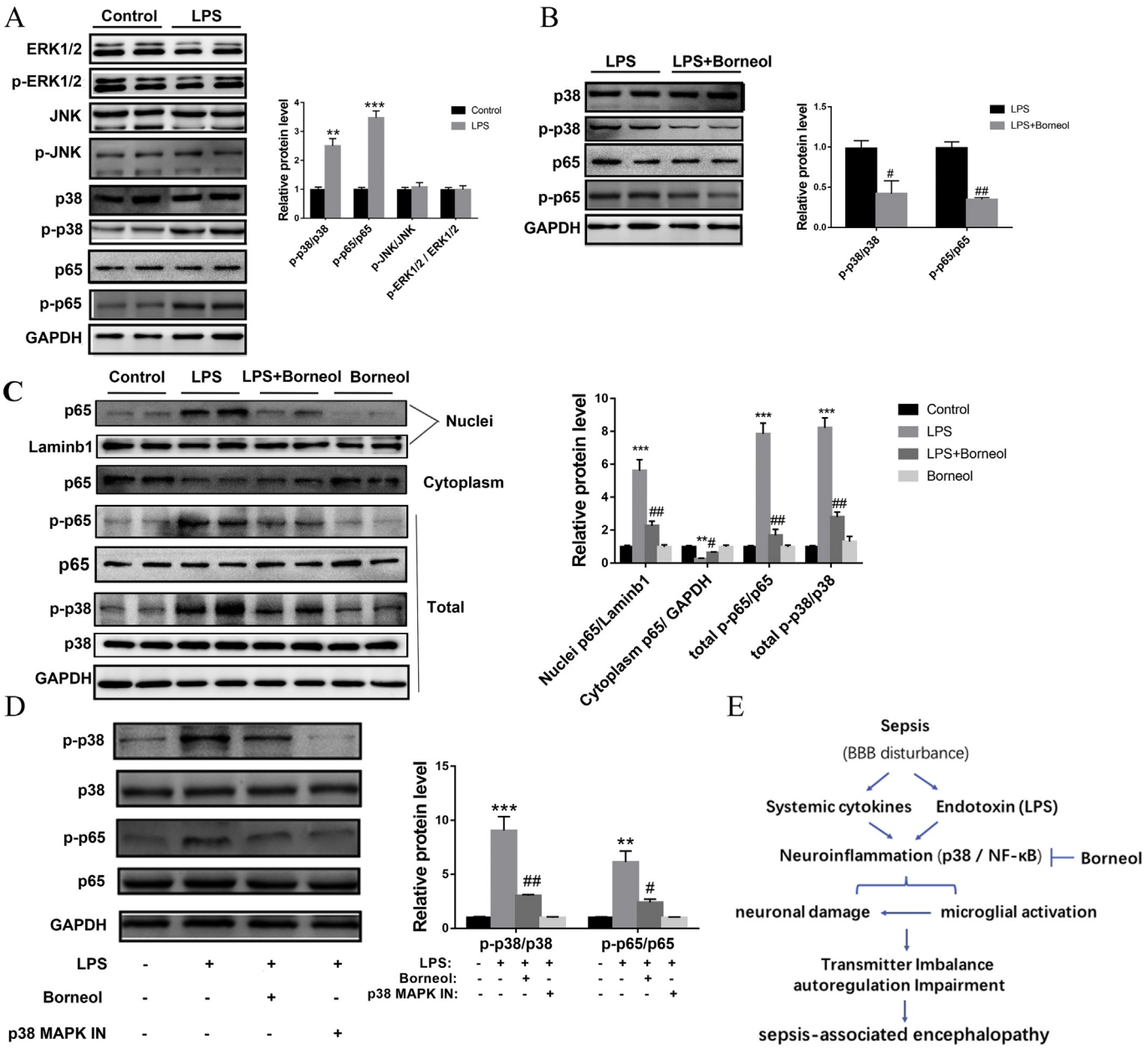

Fig. 5. Borneol suppressed neuroinflammation by inhibiting MAPK signaling. (A, B) Western blot analysis and quantifications for MAPK (p38, ERK and JNK) and NF-κB (p65) pathways in the brain cortex of mice in tested groups. (C) Western blot analysis and quantifications for p-p38/p38 and p-p65/p65 in LPS challenged (100 ng/ml, 24 h) primary microglia cells prepared from the brain cortex of day 1 or 2 mouse with or without borneol (10 μg/ml, 24 h). (D) Western blot analysis and quantifications for p-p65/p65 and p-p38/p38 expressions in cultured cortical microglia cells from day 1 or 2 new born mouse (LPS, 100 ng/ml, borneol, 10 μg/ml, p38 MAPK IN, 5 μM, all for 24 h). (E) A schematic representation of borneol's protective function. *P < 0.05, **P < 0.01, ***P < 0.001 compared with the Control group. #P < 0.05, ##P < 0.01, ###P < 0.001 compared with the LPS group.

of p38 in the brain was significantly increased after LPS challenge, while the phosphorylation of other components of MAPK pathway, ERK and JNK, were not, suggesting p38 in MAPK pathway dominating LPS response in the brain. Again, borneol suppressed LPS-induced p38 phosphorylation *in vivo*.

Similarly, in primary microglia, the phosphorylation levels of p65 and p38 were both significantly increased after LPS challenge (100 ng/ml, 24 h), which was blocked by borneol (Fig. 5C). Nucleocytoplasmic separation study showed that borneol suppressed the nucleus level of p65 that was significantly increased by LPS treatment in microglia (Fig. 5C). Interestingly, a p38 specific inhibitor p38 MAPK IN suppressed the phosphorylation levels of both p38 and p65 in microglia cells (Fig. 5D), suggesting that the phospho-p38 was required for p65 phosphorylation in the context of LPS-induced microglia activation *in vitro*. A similar result was observed in primary neurons (Supplement Figs. 3&4). Together, our results suggested that SAE characterized as neuroinflammation may include an acute and direct effect of endotoxin on cortical neurons and microglia, in addition to the persistent effect of systemic cytokines, at early stage of sepsis through p38 signaling both in neurons and microglia, which was disrupted by borneol. A schematic representation of borneol's effect is provided (Fig. 5E).

4. Discussion

Sepsis is a life-threatening condition characterized by multi-organ dysfunctions [26]. An early onset dysregulated neuronal function, or

SAE, worsens the prognosis of the condition involving an ill-neuroimmune–endocrine host response to infection [27] and an overwhelming neuronal damage [28], resulting in increased mortality of the disease or long-term impairment of brain function on sepsis survivors. Thus, blocking the progression of SAE at early stage of sepsis is essential.

Mechanistically, the pathophysiology of SAE involved the blood-brain-barrier (BBB) breakdown and systemic cytokine invasion of the brain, which triggers severe neuroinflammation [2,3]. It is suggested that during sepsis, peripheral pro-inflammatory cytokines and reactive oxygen species cause structural changes of BBB [29], leading to the activation of microglia cells and the production of cytotoxic mediators of these cells, which damages the barrier further and starts a storm of pro-inflammatory cytokines in the central nervous system (CNS) [30]. However, the possibility of direct action of bacterial endotoxin on the brain, affecting both neurons and microglia, in the early phase of sepsis should not be overlooked [31], particularly in LPS-induced sepsis models [32]. Currently, the established treatment of sepsis is mainly focusing on controlling infection and sustaining organ functions by maintaining metabolic homeostasis at systemic level [7]. However, there is a need for developing new means of neuronal protection in the early stage of sepsis. In this study, we used LPS-induced sepsis model to investigate the effect of borneol on brain protection.

Previously, borneol was suggested to suppress inflammatory response in LPS-induced acute lung injury [33] and inhibit transient receptor potential A1 (TRPA1), a proinflammatory and noxious pain-sensing cation channel [34]. Moreover, it was observed to inhibit proinflammatory cytokine release and IκBα degradation in an *in vitro* ischemic cellular model [35]. However, borneol in SAE was not studied. Herein, we found that borneol significantly reduced animal death at early stage of sepsis, tested in the male mice to avoid the influence of un-synchronized hormone on the pathogenesis of sepsis [36,37]. In parallel, borneol lessened the pro-inflammatory cytokine production and increased anti-inflammatory cytokine level in the brains of sepsis mice. The activation of microglia and neuronal damage, which is important pathological phenotype of brain injury [38], were also greatly reduced. At cellular level, borneol exhibited strong suppressive function on microglia activation and neuronal damage induced by LPS in the cultures. Thus, the early protective role of borneol on septic brain may be obtained from its action that blocked the direct toxicity of LPS on neurons and microglia.

Noted of, earlier, in contrast to more recent studies [39–43] and our work (Fig. 4) that showed a direct effect of LPS on primary cultured cerebral cortical neurons, Dr. Lehnardt [44] suggested that LPS had no direct effect on neuronal survival in the absence of microglia as cortical neurons do not express TLR4 receptor. The contradiction raised an important question that the direct effect of LPS on neurons observed in current study might be due to residual microglia or astrocyte contamination. Since a complete rejection of the possibility of microglia or astrocyte contamination is technically difficult, the conclusion, our and the others, that LPS directly acts on cortical neurons requires more rigorous work to be further confirmed. Nevertheless, neuronal expression of TLR4 in the brain and its harmful role to neuronal function were observed [45]. The remaining question is how much the direct toxic effect of LPS on neurons contributed to SAE, in compared to microglia activation, which warrants future studies. Moreover, borneol alone showed no detectable toxicity in animals and primary cells in our experimental context (Figs. 1–5), which is consistent with various previous studies [46–48].

NF-κB and MAPKs pathways were previously linked to brain injury [49] and LPS induced encephalopathy [15,16], and the members of NF-κB and MAPK pathways participated the LPS signaling cascade leading to cytokine production in macrophages and monocytes [50]. In present study, we investigated the effect of borneol on NF-κB and MAPKs activation by LPS in the brain and cells. We found that LPS activated NF-κB/p65 and p38, but not ERK or JNK signaling, which was disrupted by borneol. Finally, the p38 inhibitor p38 MAPK IN inhibited both p38 and NF-κB pathways arguing that NF-κB activation by LPS required p38 function in the context of neuron damage and microglia activation *in vivo* and *in vitro*.

5. Conclusion

The treatment of borneol alleviated brain injury at the early stage of LPS-induced sepsis by inhibiting neuroinflammation and blocking the activation of MAPK and NF-κB signaling pathways in the brain. Further, *in vitro* study indicated that this function of borneol can be achieved by suppressing the direct effect of LPS on the p38/p65 in neurons and microglia. Borneol may serve as a new agent to protect brain from septic injury in clinic.

Declaration of Competing Interest

The authors have declared that there is no conflict of interest.

Acknowledgement

The authors gratefully acknowledge the financial support of the Key Project from the National Natural Science Foundation of China (81570775).

Appendix A. Supplementary data

Supplementary data to this article can be found online at https://doi.org/10.1016/j.lfs.2019.116647.

References

[1] C.W. Seymour, F. Gesten, H.C. Prescott, et al., Time to treatment and mortality during mandated emergency care for sepsis, New Engl. J. Med. 376 (23) (2017) 2235–2244 https://doi https://doi.org/10.1056/Nejmoa1703058.
[2] T.E. Gofton, G.B. Young, Sepsis-associated encephalopathy, Nat. Rev. Neurol. 8 (10) (2012) 557–566, https://doi.org/10.1038/nrneurol.2012.183.
[3] S.C. Tauber, H. Eiffert, W. Bruck, et al., Septic encephalopathy and septic encephalitis, Expert Rev. Anti-Infect. Ther. 15 (2) (2017) 121–132, https://doi.org/10.1080/14787210.2017.1265448.
[4] T.J. Iwashyna, E.W. Ely, D.M. Smith, K.M. Langa, Long-term cognitive impairment and functional disability among survivors of severe sepsis, JAMA, J. Am. Med. Assoc. 304 (16) (2010) 1787–1794, https://doi.org/10.1001/jama.2010.1553.
[5] R.A. Balk, Severe sepsis and septic shock - definitions, epidemiology, and clinical manifestations, Crit. Care Clin. 16 (2) (2000) 179 https://doi https://doi.org/10.1016/S0749-0704(05)70106-8.
[6] C.R. Plata-Salaman, Brain injury and immunosuppression, Nat. Med. 4 (7) (1998) 768–769, https://doi.org/10.1038/Nm0798-768.
[7] E. Iacobone, J. Bailly-Salin, A. Polito, et al., Sepsis-associated encephalopathy and its differential diagnosis, Crit. Care Med. 37 (10 Suppl) (2009) S331–S336 https://doi https://doi.org/10.1097/CCM.0b013e3181b6ed58.
[8] A. Semmler, C. Frisch, T. Debeir, et al., Long-term cognitive impairment, neuronal loss and reduced cortical cholinergic innervation after recovery from sepsis in a rodent model, Exp. Neurol. 204 (2) (2007) 733–740, https://doi.org/10.1016/j.expneurol.2007.01.003.
[9] R. Kacimi, R.G. Giffard, M.A. Yenari, Endotoxin-activated microglia injure brain derived endothelial cells via NF-kappa B, JAK-STAT and JNK stress kinase pathways, J. Inflamm-Lond. 8 (2011), https://doi.org/10.1186/1476-9255-8-7 Artn 7.
[10] Y. Wu, S.J. Wang, L. Shang, H.F, et al. Effect of borneol as a penetration enhancer on brain targeting of nanoliposomes: facilitate direct delivery to neurons. Nanomedicine 2018;13(21):2709–27. https://doi.org/10.2217/nnm-2018-0282.
[11] X.G. Zhang, C. Shan, J.Z. Zhu, X.Y, et al. Additive neuroprotective effect of borneol with mesenchymal stem cells on ischemic stroke in mice. Front. Physiol. 2018;8. Artn 1133 https://doi.org/10.3389/Fphys.2017.01133.
[12] X.H. Chen, Z.Z. Lin, A.M. Liu, et al., The orally combined neuroprotective effects of sodium ferulate and borneol against transient global ischaemia in C57 BL/6J mice, J. Pharm. Pharmacol. 62 (7) (2010) 915–923, https://doi.org/10.1211/jpp.62.07.0013.
[13] J.Y. Wu, Y.J. Li, L. Yang, et al., Borneol and A-asarone as adjuvant agents for improving blood–brain barrier permeability of puerarin and tetramethylpyrazine by activating adenosine receptors, Drug Deliv. 25 (1) (2018) 1858–1864 https://doi.org/10.1080/10717544.2018.1516005.
[14] C. Liang, J. Li, Z. Zhang, et al., Suppression of mif-induced neuronal apoptosis may underlie the therapeutic effects of effective components of fufang danshen in the treatment of alzheimer's disease, Acta Pharmacol. Sin. 39 (2018) 1421–1438 https://doi https://doi.org/10.1038/aps.2017.210.

[15] F. Esen, P.E. Ozcan, E. Tuzun, et al., Mechanisms of action of intravenous immunoglobulin in septic encephalopathy, Rev. Neurosci. 29 (4) (2018) 417–423, https://doi.org/10.1515/revneuro-2017-0065.
[16] A. Agusti, O. Cauli, R. Rodrigo, et al., p38 MAP kinase is a therapeutic target for hepatic encephalopathy in rats with portacaval shunts, Gut 60 (11) (2011) 1572–1579, https://doi.org/10.1136/gut.2010.236083.
[17] B. Veres, F. Gallyas, G. Varbiro, et al., Decrease of the inflammatory response and induction of the akt/protein kinase b pathway by poly-(adp-ribose) polymerase 1 inhibitor in endotoxin-induced septic shock, Biochem. Pharmacol. 65 (8) (2003) 1373–1382 https://doi:org/10.1016/S0006-2952(03)00077-7.
[18] J. Hepatol, Y. Fang, J.F. Hu, Z.H. Wang, LncRNA H19 functions as an Aquaporin 1 competitive endogenous RNA to regulate microRNA-874 expression in LPS sepsis, Biomed, Pharmacother 105 (2018) 1183–1191, https://doi.org/10.1016/j.biopha.2018.06.007.
[19] J.A. Buras, B. Holzmann, M. Sitkovsky, Animal models of sepsis: setting the stage, Nat. Rev. Drug Discov. 4 (10) (2005) 854–865 https://doi https://doi.org/10.1038/nrd1854.
[20] T. Yi, D. Tang, F. Wang, et al., Enhancing both oral bioavailability and brain penetration of puerarin using borneol in combination with preparation technologies, Drug Deliv. 24 (1) (2017) 422–429 https://doi https://doi.org/10.1080/10717544.2016.1259372.
[21] K. Young, H. Morrison, Quantifying microglia morphology from photomicrographs of immunohistochemistry prepared tissue using ImageJ, J. Vis. Exp. 136 (2018) e57648, , https://doi.org/10.3791/57648.
[22] X. Zhang, X.L. Zhu, B.Y. Ji, et al., LncRNA-1810034E14Rik reduces microglia activation in experimental ischemic stroke, J. Neuroinflammation 16 (1) (2019) 75, https://doi.org/10.1186/s12974-019-1464-x.
[23] I. Zemtsova, B. Gorg, V. Keitel, et al., Microglia activation in hepatic encephalopathy in rats and humans, Hepatology 54 (1) (2011) 204–215 https://doi https://doi.org/10.1002/hep.24326.
[24] P.P. Tak, G.S. Firestein, Nf-kappab: a key role in inflammatory diseases, J. Clin. Invest. 107 (1) (2001) 7–11 https://doi https://doi.org/10.1172/JCI11830.
[25] R. Liu, X.Y. Liao, M.X. Pan, et al., Glycine exhibits neuroprotective effects in ischemic stroke in rats through the inhibition of M1 microglial polarization via the NF-kappaB p65/Hif-1alpha signaling pathway, J. Immunol. (2019), https://doi.org/10.4049/jimmunol.1801166.
[26] L. Bird, Inflammation hope for sepsis treatment, Nat. Rev. Drug Discov. 9 (7) (2010), https://doi.org/10.1038/nrd3212.
[27] M. Singer, V. De Santis, D. Vitale, et al., Multiorgan failure is an adaptive, endocrine-mediated, metabolic response to overwhelming systemic inflammation, Lancet 364 (9433) (2004) 545–548, https://doi.org/10.1016/S0140-6736(04)16815-3.
[28] D.L. Helbing, L. Bohm, O.W. Witte, Sepsis-associated encephalopathy, Can. Med. Assoc. J. 190 (36) (2018), https://doi.org/10.1503/cmaj.180454 E1083-E83.
[29] L.G. Danielski, A. Della Giustina, M. Badawy, et al., Brain barrier breakdown as a cause and consequence of neuroinflammation in sepsis, Mol. Neurobiol. 55 (2) (2018) 1045–1053, https://doi.org/10.1007/s12035-016-0356-7.
[30] M. Colonna, O. Butovsky, Microglia function in the central nervous system during health and neurodegeneration, Annu. Rev. Immunol. 35 (2017) 441–468, https://doi.org/10.1146/annurev-immunol-051116-052358.
[31] G. Briassoulis, P. Briassoulis, M. Miliaraki, et al., Biomarker cruises in sepsis: who is the CAPTAIN? Discussion on “Circulating biomarkers may be unable to detect infection at the early phase of sepsis in ICU patients: the CAPTAIN prospective multicenter cohort study”, Intensive Care Med. 45 (1) (2019) 132–133, https://doi.org/10.1007/s00134-018-5451-y.
[32] C.A. Moraes, G. Santos, T.C.L.D.E. Spohr, et al., Activated microglia-induced deficits in excitatory synapses through IL-1 beta: implications for cognitive impairment in sepsis, Mol. Neurobiol. 52 (1) (2015) 653–663, https://doi.org/10.1007/s12035-014-8868-5.
[33] W.T. Zhong, Y.W. Cui, Q.L. Yu, et al., Modulation of LPS-stimulated pulmonary inflammation by borneol in murine acute lung injury model, Inflammation 37 (4) (2014) 1148–1157, https://doi.org/10.1007/s10753-014-9839-8.
[34] M.A. Sherkheli, B. Schreiner, R. Haq, et al., Borneol inhibits TRPA1, a proinflammatory and noxious pain-sensing cation channel, Pak. J. Pharm. Sci. 28 (4) (2015) 1357–1363.
[35] R. Liu, L. Zhang, X. Lan, et al., Protection by borneol on cortical neurons against oxygen-glucose deprivation/reperfusion: involvement of anti-oxidation and anti-inflammation through nuclear transcription factor kappa B signaling pathway, Neuroscience 176 (2011) 408–419, https://doi.org/10.1016/j.neuroscience.2010.11.029.
[36] J. Yan, A. Mitra, J. Hu, et al., Corrigendum to interleukin-30 (il27p28) alleviates experimental sepsis by modulating cytokine profile in NKT cells, J. Hepatol. 65 (2) (2016), https://doi.org/10.1016/j.jhep.2016.04.028.
[37] C. Han, J. Jin, S. Xu, et al., Integrin cd11b negatively regulates TLR-triggered inflammatory responses by activating Syk and promoting degradation of myd88 and TRIF via CbI-b, Nat. Immunol. 11 (8) (2010) 734–742, https://doi.org/10.1038/ni.1908.
[38] M.T. Heneka, R.M. McManus, E. Latz, Inflammasome signalling in brain function and neurodegenerative disease, Nat. Rev. Neurosci. 19 (10) (2018) 610–621 https://doi https://doi.org/10.1038/s41583-018-0055-7.
[39] Y. Yang, L. Wang, Y. Wu, et al., Tanshinol suppresses inflammatory factors in a rat model of vascular dementia and protects lps-treated neurons via the mst1-foxo3 signaling pathway, Brain Res. 1646 (2016) 304–314 https://doi https://doi.org/10.1016/j.brainres.2016.06.017.
[40] R.E. Miller, A. Belmadani, S. Ishihara, et al., Damage-associated molecular patterns generated in osteoarthritis directly excite murine nociceptive neurons through toll-like receptor 4, Arthritis Rheumatol. 67 (11) (2015) 2933–2943 https://doi https://doi.org/10.1002/art.39291.
[41] M. Zhao, A. Zhou, L. Xu, et al., The role of tlr4-mediated pten/pi3k/akt/nf-κb signaling pathway in neuroinflammation in hippocampal neurons, Neuroscience 269 (2014) 93–101 https://doi https://doi.org/10.1016/j.neuroscience.2014.03.039.
[42] J.L. Lai, Y.H. Liu, C. Liu, et al., Indirubin inhibits lps-induced inflammation via tlr4 abrogation mediated by the NF-kB and MAPK signaling pathways, Inflammation 40 (1) (2017) 1–12 https://doi https://doi.org/10.1007/s10753-016-0447-7.
[43] J.C. Fehrenbacher, C. Guo, M.R. Kelley, et al., DNA damage mediates changes in neuronal sensitivity induced by the inflammatory mediators, MCP-1 and LPS, and can be reversed by enhancing the dna repair function of ape1, Neuroscience 366 (2017) 23 https://doi https://doi.org/10.1016/j.neuroscience.2017.09.039.
[44] S. Lehnardt, L. Massillon, P. Follett, et al., Activation of innate immunity in the cns triggers neurodegeneration through a toll-like receptor 4-dependent pathway, Proc. Natl. Acad. Sci. U. S. A. 100 (14) (2003) 8514–8519 https://doi https://doi.org/10.1073/pnas.1432609100.
[45] S.C. Tang, T.V. Arumugam, X. Xu, et al., Pivotal role for neuronal toll-like receptors in ischemic brain injury and functional deficits, Proc. Natl. Acad. Sci. U. S. A. 104 (34) (2007) 13798–13803 https://doi https://doi.org/10.1073/pnas.0702553104.
[46] S.P. Bhatia, C.S. Letizia, A.M. Api, Fragrance material review on borneol, Food Chem. Toxicol. 46 (11) (2008) S77–S80 https://doi https://doi.org/10.1016/j.fct.2008.06.031.
[47] E. Horváthová, K. Kozics, A. Srančíková, et al., Borneol administration protects primary rat hepatocytes against exogenous oxidative DNA damage, Mutagenesis 27 (5) (2012) 581 https://doi https://doi.org/10.1093/mutage/ges023.
[48] C. Cheng, X. Liu, F. Du, et al., Sensitive assay for measurement of volatile borneol, isoborneol, and the metabolite camphor in rat pharmacokinetic study of borneolum (bingpian) and borneolum syntheticum (synthetic bingpian), Acta Pharmacol. Sin. 34 (10) (2013) 1337–1348 https://doi https://doi.org/10.1038/aps.2013.86.
[49] Y. He, N.A. Jackman, T.L. Thorn, et al., Interleukin-1 protects astrocytes against oxidant-induced injury via an NF-B-dependent upregulation of glutathione synthesis, Glia 63 (9) (2015) 1568–1580 https://doi https://doi.org/10.1002/glia.22828.
[50] T.H. Page, A. Brown, E.M. Timms, et al., Inhibitors of p38 suppress cytokine production in rheumatoid arthritis synovial membranes does variable inhibition of Interleukin-6 production limit effectiveness *in vivo*? Arthritis Rheum. 62 (11) (2010) 3221–3231 https://doi https://doi.org/10.1002/art.27631.